Role of Tyrosine-103 in Myoglobin Peroxidase Activity: Kinetic and Steady-State Studies on the Reaction of Wild-Type and Variant Recombinant Human Myoglobins with H_2O_2†

Paul K. Witting,*,‡,§ A. Grant Mauk,|| and Peter A. Lay⊥

Biochemistry Group, The Heart Research Institute, 145 Missenden Road, Camperdown, Sydney, Australia 2050, Department of Biochemistry and Molecular Biology, University of British Columbia, Vancouver, British Columbia, Canada, and School of Chemistry, University of Sydney, NSW, Australia 2006

Received March 18, 2002; Revised Manuscript Received July 26, 2002

ABSTRACT: Myoglobin (Mb) catalyzes a range of oxidation reactions in the presence of hydrogen peroxide (H_2O_2) through a peroxidase-like cycle. C110A and Y103F variants of human Mb have been constructed to assess the effects of removing electron-rich oxidizable amino acids from the protein on the peroxidase activity of Mb: a point mutation at W14 failed to yield a viable protein. Point mutations at C110 and Y103 did not result in significant changes to structural elements of the heme pocket, as judged by low-temperature electron paramagnetic spectroscopy (EPR) studies on the ground-state ferric proteins. However, compared to the native protein, the yield of globin radical (globin•) was significantly decreased for the Y103F but not the C110A variant Mb upon reaction of the respective proteins with H_2O_2. In contrast with our expectation that inhibiting pathways of intramolecular electron transfer may lead to enhanced Mb peroxidase activity, mutation of Y103 marginally decreased the rate constant for reaction of Mb with H_2O_2 (1.4-fold) as judged by stopped-flow kinetic analyses. Consistent with this decrease in rate constant, steady-state analyses of Y103F Mb-derived thioanisole sulfoxidation indicated decreased V_{max} and increased K_m relative to the wild-type control. Additionally, thioanisole sulfoxidation proceeded with lower stereoselectivity, suggesting that Y103 plays a significant role in substrate binding and orientation in the heme pocket of Mb. Together, these results show that electron transfer within the globin portion of the protein is an important modulator of its stability and catalytic activity. Furthermore, the hydrogen-bonding network involving the residues that line the heme pocket of Mb is crucial to both efficient peroxidase activity and stereospecificity.

Peroxidase enzymes are a ubiquitous class of hemoproteins that perform a wide range of biological function (*1*). Peroxidases catalyze the oxidation of various biological molecules by degrading hydroperoxides (often H_2O_2) (*1*). In this catalytic cycle, the iron (Fe[III]) center of the resting state reacts with 2 mol of H_2O_2 to generate a porphyrin radical cation (Compound I). In the presence of a suitable substrate (AH_2), Compound I is reduced through a one-electron process to yield Compound II. Compound II oxidizes AH_2 to regenerate the resting enzyme.

$$\text{protein-heme(Fe[III])} + H_2O_2 \xrightarrow{k_1} \text{Compound I} + H_2O$$
$$\text{Compound I} + AH_2 \xrightarrow{k_2} \text{Compound II} + AH^\bullet$$
$$\text{Compound II} + AH_2 \xrightarrow{k_3} \text{protein-heme(Fe[III])} + AH^\bullet$$

The structure, function (*2*), and kinetic properties (*3*) of peroxidases have been studied extensively to provide a framework for molecular engineering approaches to alter substrate specificity (*4*) and increase both thermal stability (*5*) and catalytic activity (*6*) of the protein.

Myoglobin (Mb)[1] is an intracellular hemo-protein found in skeletal, cardiac (*7*), and smooth muscle (*8*). Mb shares many physical, spectroscopic, and chemical similarities with authentic peroxidases. For example, ferric or metmyoglobin (metMb) has a limited ability to reduce H_2O_2 to water with the concomitant formation of ferryl [Fe(IV)=O] heme and a porphyrin radical cation (*9*). The reaction of metMb with H_2O_2 also yields protein radicals (globin•) (*10*) through heterolytic cleavage of the peroxide (*11*). The identity of the Mb residue(s) that form globin• in the presence of H_2O_2 has been the subject of some controversy. The precise location of the radical on the protein is likely to be dependent on both the mechanism by which it forms and the stability of the radical (*12*). Globin• have been assigned to occur at tyrosine (Y103 and Y146) (*13*, *14*) and/or tryptophan (W14) (*15*) residues through the use of electron paramagnetic

† This work was supported by Grant O 98S 0008 from the National Heart Foundation of Australia (to P.K.W.) and CHIR Grant MT-7182 (to A.G.M.). The stopped-flow instrument was purchased with the support of an Australian Research Council Grant (to P.A.L.).

* To whom correspondence should be addressed.

‡ The Heart Research Institute.

§ Current address: The Centre for Thrombosis and Vascular Research, School of Medical Science, University of New South Wales, UNSW Sydney 2052. Phone: 61-2-9385-1377, Fax: 61-2-9385-1389, E-mail: p.witting@unsw.edu.au.

|| University of British Columbia.

⊥ University of Sydney.

[1] Abbreviations: C110, cysteine at position 110; C110A, cysteine-110 to alanine variant of human Mb; DTPA, diethylenetriaminepentaacetic acid; EPR, electron paramagnetic resonance spectroscopy; globin•, protein radicals; Mb, myoglobin; metMb, metmyoglobin; Y103, tyrosine at position 103; Y103F, tyrosine-103 to phenylalanine variant of human Mb; W14-OO•, tryptophan-14 peroxyl radical.

10.1021/bi025835w CCC: $22.00
Published on Web 08/30/2002

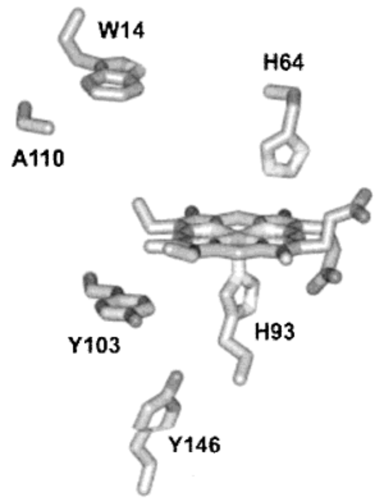

FIGURE 1: Structural elements of the heme pocket from the K45R/C110A variant of human Mb. Proximal and distal histidine residues of the protein are shown below and above the plane of the heme prosthetic group, respectively. Other critical residues are included to show proximity to the heme group. Wild-type human Mb contains C110 in place of A110.

spectroscopy (EPR). The transfer of oxidizing equivalents to amino acids adjacent to the heme prosthetic group (to yield globin•) decreases Mb peroxidase activity (*16*). Thus, understanding the role of specific amino acids within the Mb active site may lead to the development of molecular engineered proteins with enhanced catalytic activity (*6*, *17*, *18*) for commercial applications (*19*).

The role of Mb as a short-term reservoir of O_2 is well established. Mb facilitates O_2 transfer from the extracellular matrix into the cell cytosol by translational diffusion, releasing O_2 in a cycle termed "facilitated O_2-diffusion" (*20*, *21*). However, generation of viable transgenic mice deficient in Mb conflicts with this physiological role for Mb (*22*). Interestingly, the loss of Mb results in multi-compensatory mechanisms invoking nitric oxide (•NO) chemistry (*23*, *24*). These latter observations have shifted the focus for Mb from O_2 transport to a role in •NO homeostasis (*25*). In support for this idea, •NO oxidation by oxy-Mb modulates intracellular concentrations of the signal molecule in cardiac myocytes (*15*): regulation of myocardial •NO is crucial for maintaining coronary blood flow, cardiac contractility, and normal heart function. Human Mb is similar in sequence to other mammalian myoglobins except for the presence of a cysteine residue at position 110 (C110) (*27*). Reaction of wild-type human Mb and H_2O_2 yields globin• derived from tryptophan-14 (W14), tyrosine (Y103 and Y146, respectively), and cysteine (C110) (*28*). Reaction of C110 in human Mb with •NO yields *S*-nitroso-Mb (*29*), and this may prove to be a pool of bio-active •NO.

The three-dimensional structure of wild-type human Mb has not been reported. An alternate structure for estimating distances between structural elements of this protein is the crystal structure of the K45R/C110A variant of human Mb (*27*). In this structure, determined at 2.8 Å resolution, Y103 is the tyrosine residue nearest the heme group, as is also the case for sperm whale (*30*) and horse heart (*31*) Mb (Figure 1): the point of closest approach is a phenyl carbon that is ~3.44 Å from the edge of the heme group. Studies of the reaction of the Y103F variant of human Mb and H_2O_2 indicated that Y103 was involved in the translocation of oxidizing equivalents to the protein yielding C110-derived thiyl radicals (*32*). Together, these observations support the idea that substitution of Y103 by an oxidation-inert amino acid (phenylalanine) should enhance the catalytic activity of Mb. Herein, we report kinetic and steady-state investigations of the reactions of wild-type Mb and C110A and Y103F variants of recombinant human Mb with H_2O_2, and establish that Y103 plays an important role in substrate orientation as well as influencing the rate of peroxide degradation.

EXPERIMENTAL PROCEDURES

Materials. Trypsin (type III, 10 200 units/mg of protein), urea, EDTA, TEMPO, diethylenetriaminepentaacetic acid (DTPA), 2-butanone, acetaphenone (purity >99%), and thioanisole (99% purity) were obtained from Sigma (Sydney, Australia). Racemic thioanisole sulfoxide (>97% purity) was from Aldrich (Sydney, Australia). Tryptone and yeast extract were from Bectin Dickinson (Sparks, MD). Dithiothreitol and NaCl were obtained from Fisher Scientific (Fair Lawn, NJ). Hydrogen peroxide (H_2O_2) was from BioRad (Richmond, CA). Buffers were prepared from either glass-distilled water or glass-distilled water that was purified further by passage through a Barnstead Nanopure system. Buffers were stored over Chelex-100 (BioRad) at 4 °C for 24 h to remove contaminating transition metals as verified by the ascorbate autoxidation assay (*33*). Solvents and all other chemicals employed were of the highest quality available.

Site-Directed Mutagenesis. Restriction enzymes were from New England Biolabs or Gibco BRL. DNA manipulations were performed using procedures described in (*34*). Complementary oligomers were synthesized and DNA sequence analysis was performed at the UBC Nucleic Acid and Protein Services Unit (University of British Columbia, Canada). Site-directed mutagenesis was performed with the pBluescript II KS(±) vector (Stratagene, La Jolla, CA). DNA was amplified by the polymerase-chain reaction with a high-fidelity Pfu-Turbo DNA polymerase (Stratagene). Point mutations were confirmed by DNA sequence analysis prior to protein expression in bacteria. Once the sequence was confirmed, the *Bam*HI−*Hin*dIII fragment from the amplified DNA, which also contained the mutant Mb coding, was ligated to the *Bam*HI−*Hin*dIII fragment from the vector pMb*3* (*35*) to yield the final expression vector. The circular plasmid was then transformed to the appropriate cell line for protein expression. Thus, DNA bearing the Y103F mutation was obtained by site-directed mutagenesis and used to transform *Escherichia coli* DH10B cells (see below). DNA bearing the W14FY103F double mutation consistently ($n = 3$) yielded a sequence in which one base had been deleted, effectively scrambling the sequence (i.e., a DNA frame-shift), while DNA bearing the W14F single point mutation failed to yield protein upon transformation into DH10B cells (not shown).

Preparation of Recombinant Protein. Transformed *E. coli* (strain AR68) containing plasmids for both the wild-type recombinant human myoglobin and the C110A variant (*35*) were obtained from Prof. S. G. Boxer (Stanford University). For transformed bacteria (strain AR68), cells were grown at 28 °C in 10 × 2 L flasks containing 2YT super-broth (1 L per flask: tryptone 16 g/L, yeast extract 10 g/L, and NaCl 5 g/L) to an optical density (OD_{600nm}) of 1.2−1.5. The expression of recombinant Mb proteins was induced by immersing each flask into a water bath (55 °C) for 5 min and then transferring the flask to an incubator operating at 42 °C. For the case of transformed DH10B cells, cultures were grown at 28 °C in 10 × 2 L flasks containing 2YT super-broth to OD_{600nm} ∼3−4, and then the heat shock was applied in a fashion similar to that described for transformed AR68 cells. All cultures were subsequently incubated for a further 6−7 h, and the cells were harvested. Rapidly increasing the culture temperature in this manner was essential, as simply increasing the incubation temperature from 28 to 42 °C failed to induce protein expression. Where relevant, Mb (isolated as a fusion product) was purified by anion-exchange chromatography (DE52 resin, Whatman) as described (*35*). The fusion protein(s) was (were) reconstituted with excess hemin (heme:protein ratio ∼1.5) (Porphyrin Products, Logan, UT), treated with trypsin (final concentration ∼0.1 μg/mL) to cleave the fusion segment, and then further purified as described previously (*35*). Thus, recombinant Mb was isolated as metMb. When required, proteins were concentrated by ultra-filtration (Centriprep-10 concentrators, Millipore). Each ferric protein showed an A_{Soret}/A_{280nm} ratio >5, consistent with the high purity of each preparation (not shown).

EPR Spectroscopy. X-band EPR spectra were obtained with a Bruker EMX Benchtop spectrometer. Mb solutions (0.5 mM) were treated with H_2O_2 (H_2O_2:protein ratio ∼1.2 or 5). A sample of the reaction mixture (250 μL) was removed and transferred into a standard quartz round cell (Wilmad, Buena, NJ), snap-frozen in liquid N_2, and transferred to a finger-dewar insert (77 K) for EPR analyses. The limit of detection of a stable nitroxide (TEMPO) measured under identical conditions was determined to be ∼50 nM. EPR spectra were obtained as an average of 3−5 scans with a modulation frequency of 100 kHz and a sweep time of 84 s. Microwave power, modulation amplitude, and scan range used for each analysis varied appropriately as indicated in the figure legends. Radical concentrations were determined by peak area comparison with that from a 10 mM solution of TEMPO measured under identical spectrometer conditions. Peak areas were assessed by double integration with WINEPR software (Bruker). DTPA (100 μM) was included in reaction mixtures to minimize the possibility of peroxide decomposition by Fenton-type chemistry.

Sulfoxidation of Thioanisole. Solutions of Mb (50 μM final protein concentration) were treated with acetaphenone (50 μM), and then thioanisole was added to the final concentrations indicated in the figure legends. Thioanisole was not miscible in the reaction buffer above 3 mM, so investigations were limited to [thioanisole] ≤ 2.5 mM. Sulfoxidation was initiated in these mixtures by addition of H_2O_2 (*36*) at a H_2O_2:Mb ratio of ∼10 mol/mol. DTPA (100 μM) was included in all reaction mixtures prior to H_2O_2 addition. After incubation at 37 °C for 1 h, reaction mixtures were extracted into CH_2Cl_2 (2 × 5 reaction volumes). The combined organic phase was evaporated to dryness (under a flow of N_2 gas), and the residue was suspended in hexane/isopropyl alcohol (4:1 v/v) for analyses. Sulfoxides present in the extract were then analyzed by HPLC with a chiral column (Chiralcel OD-H, Diacel Chemical Industries) with hexane/2-propanol (4:1 v/v) as eluent and monitoring at 254 nm (*36*). Concentrations of acetaphenone and sulfoxide products were determined by peak area comparison with authentic standards. Total yields of sulfoxide [*R*(+) and *S*(−)] were corrected for acetaphenone recovery and used for determinations of reaction velocity. Assignment of identity to the sulfoxide products was performed by polarimetry using an Optical Activity (Polaar 2001) polarimeter. Thus, a solution of isolated thioanisole sulfoxide with a retention time of ∼21−22 min (purity 94%) gave an observed rotation $\alpha_{obs(ethanol)}$ = (+) 2.7 ± 0.2° (mean ± SD, $n = 3$) and was assigned as the *R*(+)-sulfoxide.

Peroxidase Kinetics. Kinetic determinations for the reactions of wild-type and Y103F variant forms of human Mb with H_2O_2 were performed with an Applied Photophysics SX-17 MV stopped-flow spectrophotometer. Typically, 250 time-dependent spectra (logarithmic time-base, integration 2.56 ms, dead-time ∼2 ms, λ = 350−750 nm, resolution 1 nm) were collected over 100 s at 25 °C. Kinetic data were processed using Pro-Kineticist global analysis software (Pro-Kineticist, Version 4.1; Applied Photophysics, Leatherhead, U.K., 1996), as described previously (*37*). Apparent rate constants (k_1) were then determined by linear regression.

Electronic spectra were measured with a Cary 3E UV/Vis spectrophotometer. Spectra of the Y103F and C110A variants prepared in phosphate buffer (50 mM, pH 7.4) showed Soret (λ_{max} = 409 nm) and visible bands (λ_{max} = 505−508 and 630−633 nm) similar to those of native Mb (*32*) (not shown). These spectral features are consistent with a hexa-coordinate high-spin ferric form of heme (*38*). Where required, Mb solutions were quantified with $\epsilon_{409nm} \sim 153 \times 10^3$ M^{-1} cm^{-1} (*39*).

Where required, heme-free Mb apoprotein was prepared by adjusting the pH of solutions of the respective holo-Mb in phosphate buffer (50 mM, pH 7.4) to pH 2.5 by addition of 1 M HCl at 4 °C. Free heme was then removed from the mixture by repeated extraction (×3) of the acidified fraction into ice-cold 2-butanone as described previously (*40*). The acidified aqueous fraction was then dialyzed against phosphate buffer (50 mM, pH 7.4 containing 100 μM DTPA), and the concentration of apo-Mb was determined using $\epsilon_{280nm} = 16 \times 10^3$ M^{-1} cm^{-1}).

Statistical Analyses. Statistics were performed with the Student's *t*-test available in MS Excel (Microsoft), and statistical significance accepted the 95% confidence level ($P < 0.05$).

RESULTS

Electron Paramagentic Resonance Spectroscopy. EPR spin-trapping investigations on globin• generated through reaction of Y103F and H_2O_2 have established that the mutation efficiently decreased the radical density on the protein (*32*). However, one limitation of these spin-trapping studies is the requirement that globin• and added trap must react at close proximity to yield a radical-adduct. Therefore, it remains a possibility that radical species formed on human Mb may remain inaccessible to the added spin trap. Also, reaction of H_2O_2 with the W14F/Y146F/Y103F/K102Q variant of sperm whale Mb failed to inhibit globin• formation, indicating that yet other amino acids were involved in globin• generation on Mb (*41*). For example, H64 in Mb is implicated as an intramolecular reducing agent that reacts with the intermediate porphyrin radical cation to decrease Mb peroxidase activity (*23*, *42*).

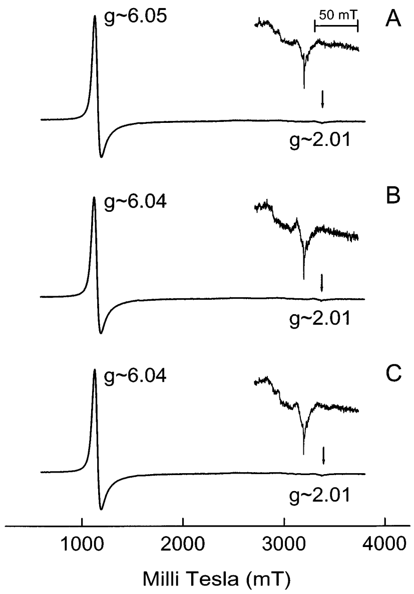

FIGURE 2: Ground-state EPR spectra obtained for 0.5 mM solutions of (A) wild-type human Mb and the (B) C110A and (C) Y103F variants of human Mb at 77 K. Where appropriate, g values are indicated on the figures. Insets show spectra measured with the scan width expanded in the $g \sim 2$ region of the field (arrow) for the respective proteins. Parameters: power, 3 mW; frequency, 9.49 GHz; modulation amplitude, 0.2 mT; gain, 1×10^5; scan time, 168 s; and time constant, 164 ms. Data are representative of 3 independent analyses with different Mb preparations.

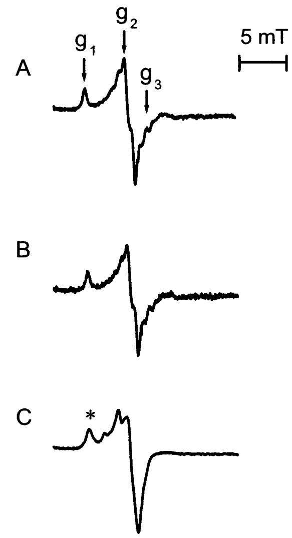

FIGURE 3: W14-OO$^\bullet$ radicals are detected in reaction mixtures containing (A) wild-type human Mb and (B) C110A and (C) Y103F variants of human Mb and H_2O_2. Solutions of Mb (final concentration 0.5 mM) were treated with H_2O_2 (H_2O_2:Mb ~5 mol/mol) and immediately frozen in liquid N_2, and the reactions were monitored by EPR in the $g \sim 2$ region of the field at 77 K. Peak response g shifted to $g_1 \sim 2.036$ (asterisk in Figure 3C) is typical of a radical localized to a heteroatom (*59*). Parameters: power, 1.3 mW; frequency, 9.49 GHz; modulation amplitude, 0.1 mT; gain, 2×10^5; sweep time, 83 s; and time constant, 164 ms. Panels A−C are presented with identical intensity scales. Data presented are representative of 3 independent analyses with different Mb preparations.

Therefore, we investigated the EPR response for wild-type and variant Mb's in the absence or presence of H_2O_2 without an added spin trap and at 77 K. In the absence of H_2O_2, frozen Mb solutions showed signals at $g \sim 6$ and $g \sim 2$ assigned as the $g_\perp$ and $g_\parallel$ signals of ferric high-spin iron, respectively (Figure 2). Ground-state EPR spectra obtained for the C110A and Y103F variants showed no significant differences from those of the wild-type protein (cf. Figure 2A−C and their respective insets).

Addition of H_2O_2 (H_2O_2:Mb ~5 mol/mol) eliminated the signal at $g \sim 6$ (data not shown), and globin$^\bullet$ radicals were observed by EPR as judged by the changes in the $g \sim 2$ region of the field (Figures 3 and 4). Globin$^\bullet$ radicals on wild-type and C110A Mb proteins detected immediately after H_2O_2 treatment were identical (cf. Figure 3A,B): peak response(s) centered at $g_1 \sim 2.036$, $g_2 \sim 2.013$, and $g_3 \sim 2.006$ were consistent with the formation of a W14 peroxyl radical (W14-OO$^\bullet$) on Mb (*22*, *43*). In contrast, reaction of the Y103F variant and H_2O_2 generated a mixture of radicals (Figure 3C). Clearly, the peak g shifted to $g_1 \sim 2.036$ is similar to that for the corresponding reactions of wild-type Mb and C110A Mb with peroxide. However, the signal centered at $g \sim 2.01$ is complex and suggestive of closely overlapping signals from a mixture of radicals. Incubation of either the wild-type Mb or the C110A variant Mb with H_2O_2 at 77 K resulted in decay of the signal at g_1 and broadening of the g_2 signal over 30 s (Figure 4A,B). Such broad, poorly resolved peak responses have been assigned previously to a mixture of Y103 and Y146 tyrosyl phenoxyl radicals on horse heart (*43*) and human Mb (*28*), respectively. Incubation of Y103F Mb with H_2O_2 at 77 K resulted in decay of the signal at $g \sim 2.036$ and detection of a multiplet EPR signal (cf. Figures 3C and 4C). The yields of globin$^\bullet$ radicals determined in reactions of Y103F Mb and H_2O_2 after decay of the W14-OO$^\bullet$ were consistently lower (by a factor ~42%) than in corresponding reactions of the wild-type protein. In the absence of protein, no EPR signal was detected (Figure 4D), indicating that the radical signals detected in the $g \sim 2$ region were not simply due to a dewar artifact. Where investigated, signals detected after the W14-OO$^\bullet$ decay were stable for up to 15 min of monitoring at 77 K. No other radicals were detected over this time (not shown).

Cross-Linking of Heme to the Apoprotein of Human Mb. Following formation of ferryl Mb, a proportion of heme is irreversibly cross-linked to the protein via reaction with Y103-derived phenoxyl radicals (*44*). Therefore, the formation of cross-linked heme (*45*, *46*) can be employed as a surrogate measure of globin$^\bullet$ formation on Mb. Treatment of wild-type Mb and either C110A or Y103F variant Mb's with peroxide, followed by removal of heme (*40*), afforded the corresponding apo-Mb containing varying concentrations of cross-linked heme as judged by a residual absorbance at A_{409nm} (not shown). Incubation of wild-type Mb or the C110A variant Mb with H_2O_2 resulted in a significant increase of residual heme compared with the corresponding apo-Mb in the absence of peroxide treatment (Table 2). In contrast, mutation of Y103 decreased the concentration of residual heme and, therefore, the extent of heme cross-linking compared to the native protein under identical conditions (Table 2). Together, these data confirm that Y103 is the site for covalent binding of the heme prosthetic group in human Mb similar to the situation in sperm whale Mb (*44*), and support the argument that mutation of Y103 significantly decreases the yield of globin$^\bullet$ on human Mb.

Reactions of Ferric Myoglobins with Peroxide. The pK_a value for the acid−base transition in the Y103F variant (8.26

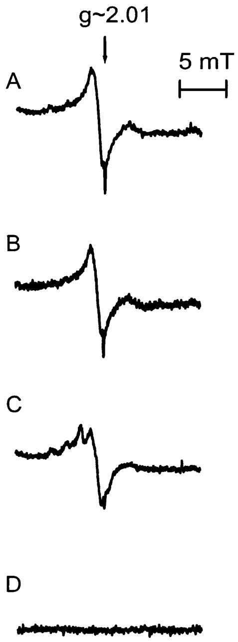

FIGURE 4: Solutions containing (A) wild-type human Mb, (B) C110A and (C) Y103F variants of human Mb, or (D) buffer alone were treated with H_2O_2 (as described in the legend to Figure 3). Panels A−C show the EPR spectra obtained after incubating the samples for 10 min at 77 K to facilitate the decay of W14-OO$^{\bullet}$ as judged by the decay of the peak *g* shifted to $g \sim 2.036$. Globin$^{\bullet}$ radical concentration was determined to be 0.13 ± 0.03 spin/mol of protein in panels A and B, while in panel C the spin density was determined to be 0.05 ± 0.03 spin/mol of Mb. EPR parameters were as for Figure 3. Data presented are representative of 3 independent analyses using different Mb preparations.

Table 1: Apparent Rate Constants for the Reaction of Various Heme-proteins with H_2O_2 [a]

protein	k_1 (M^{-1} s^{-1})	source
wild-type human Mb	$3.2 (0.2) \times 10^2$	present study
wild-type human Mb	2.7×10^2	(*48*)
C110A Mb	$3.5 (0.2) \times 10^2$	present study
Y103F Mb[b]	$2.3 (0.1) \times 10^2$	present study
HRP	2.0×10^7	(*53*)
cytochrome *c* peroxidase	5.0×10^7	(*63*)

[a] Reactions were performed in 50 mM phosphate buffer (pH 6) maintained at 25 °C and with Mb (final concentration 5 μM) and H_2O_2 concentrations ranging from 0.005 to 1 mM. Where possible, kinetic data (k_1) are reported as the mean ± SD of ≥3 independent analyses. [b] Significantly different from the corresponding value for wild-type Mb or C110A variant Mb ($P < 0.05$).

± 0.03) is significantly lower than that determined for the wild-type protein (8.29 ± 0.09) (*32*). Because the conversion from ferric aquo to ferric hydroxo decreases the rate of Mb reaction with peroxides (*47*), we chose reaction conditions to eliminate the acid−base transition as a confounding factor in the kinetic analyses. Therefore, rapid-scan analyses of mixtures of the Y103F variant and H_2O_2 were performed in phosphate buffer (50 mM, pH 6) and resulted in the time-dependent changes to the electronic spectra indicated (Figure 5A). Independent of the Mb employed, mixing protein and H_2O_2 resulted in decreases in peak intensities at A_{409nm}, A_{505nm}, and A_{633nm}, and concomitant increases in A_{420nm}, A_{550nm}, and A_{585nm} values. These changes in spectral properties are consistent with formation of an iron(IV)-oxo (or ferryl Mb) derivative (*16*). Kinetic analyses of these stopped-flow transient-kinetic traces showed a monophasic decrease in the

Table 2: Cross-Linked Heme Present after the Reaction of Various Mb Proteins with H_2O_2 [a]

protein	holo-Mb/apo-Mb ratio (%) before H_2O_2 addition	holo-Mb/apo-Mb ratio (%) after H_2O_2 addition	residual [cross-linked heme] (μM)
wild-type human Mb	2.1 (0.3)	8.5 (0.5)[b]	1.1
C110A Mb	0.9 (0.2)	7.2 (2.0)[b]	1.1
Y103F Mb	1.3 (0.1)	2.0 (0.8)[c]	0.03

[a] Proteins were incubated in the presence or absence of added H_2O_2 (where relevant at Mb:H_2O_2 ~5 mol/mol) for 15 min at 37 °C; then the reaction mixture was acidified and free heme was extracted as described previously (*40*). The fraction of holo-Mb/apo-Mb (representing residual heme) was determined from the percentage ratio for A_{409nm}/A_{260nm}. The concentration of cross-linked heme was determined from the residual A_{409nm} [$\epsilon_{409nm} \sim 153 \times 10^3$ M^{-1} cm^{-1} (*39*)] remaining from 3 consecutive extraction procedures. Data represent the mean ± SD from 3 independent analyses using different Mb preparations. [b] Significantly different from the corresponding holo-Mb/apo-Mb ratio before peroxide treatment ($P < 0.05$). [c] Significantly different from wild-type and C110A variant Mb proteins after peroxide treatment ($P = 0.001$).

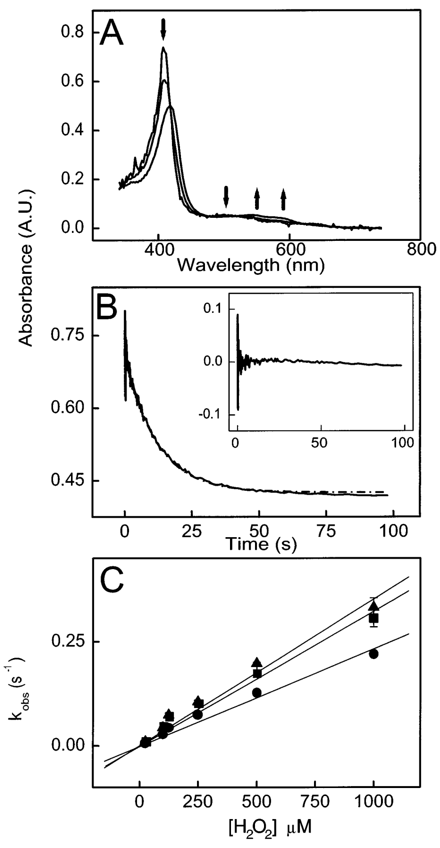

FIGURE 5: Stopped-flow rapid-scan electronic spectra obtained upon mixing native human Mb (5 μM final concentration) with H_2O_2. (A) Reactions were performed in phosphate buffer (50 mM, pH 6) at 25 °C, and the time-dependent transformation of metMb to ferryl Mb was monitored over 100 s. (B) Single-exponential fit (broken line) of the monophasic decay measured at A_{409nm} (filled line) yields a low residual (B, inset). (C) Plots of the observed rate constants (k_{obs}) versus [H_2O_2] were readily fitted by linear regression to yield the apparent rate constant k_1 as the slope of the line. Data are presented as the mean ± SD of 3 independent analyses. Where error bars are not shown, the symbol is larger than the error.

value of A_{409nm} (Figure 5B). This decay curve was readily simulated with a single-exponential function (Figure 5B, dashed line and inset). Pseudo-first-order rate constants (k_{obs})

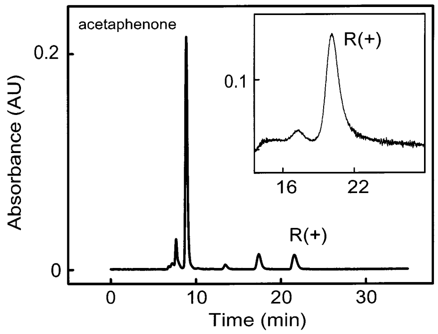

FIGURE 6: Representative chromatogram showing the reaction products of Mb/H_2O_2-mediated thioanisole sulfoxidation after 1 h at 37 °C (figure taken from a mixture of thioanisole, Y103F Mb, and peroxide at 5:1:2 mol/mol/mol). Peak eluting with retention time 9.2 min corresponds to the internal standard (acetaphenone), while peaks at ∼17−18 and 21−22 min are the *S*(−)- and *R*(+)-sulfoxide products, respectively. The inset shows the chromatogram obtained from a purified sample of *R*(+)-thioanisole sulfoxide employed in polarimetry studies. HPLC conditions are as described under Experimental Procedures.

were calculated from the global analysis fit and plotted against increasing H_2O_2 concentration as described (*48*) to afford linear relationships for all proteins tested (Figure 5C). The data presented in Table 1 summarize the k_1 values for the reaction of the various Mb proteins with peroxide together with reported data for wild-type human Mb and other authentic peroxidase enzymes. The values of k_1 for reactions of wild-type and the C110A variant human Mb proteins with H_2O_2 were similar; however, they were 5−6 orders of magnitude lower than the corresponding k_1 values from horseradish (HRP) or cytochrome *c* peroxidase. Importantly, the k_1 values that were determined from reactions of wild-type human Mb and peroxide in this present study are similar to that previously reported for this recombinant protein (Table 1), thereby verifying our data. In contrast with the expectation that decreased globin$^\bullet$ yield on Y103F Mb increases catalytic activity, the k_1 value was consistently lower (1.4-fold) than for wild-type and C110A proteins. These data are *incongruous* with the idea that simple translocation of oxidizing equivalents to globin is a major pathway leading to decreased Mb peroxidase activity.

Thioanisole Sulfoxidation. For reactions of authentic peroxidase and H_2O_2, the two-electron oxidation product of the native enzyme is stable and can be detected directly by electronic absorption spectroscopy. However, for the case of Mb an authentic Compound I has not been characterized (*49*) likely due to rapid formation of globin$^\bullet$ radicals [for a conflicting view, refer to (*50*)]. Importantly, through the ability for peroxidase proteins to receive 2 oxidizing equiv more than the resting Fe[III] enzyme, the corresponding Compound I product can act as a peroxygenase. Therefore, the determination of Mb peroxygenase activity can be considered as a surrogate to indirectly assess the effect of amino acid modification on Mb peroxidase activity.

In the presence of Mb/H_2O_2, thioanisole was oxidized to yield a mixture of sulfoxides that were readily resolved by HPLC (e.g., Figure 6). Consistent with reported data for thioanisole sulfoxidation induced by other mammalian Mb (*25, 42*), human Mb oxidized thioanisole with reasonable stereoselectivity with the *R*(+) enantiomer formed in excess over the *S*(−) enantiomer (Table 3). In contrast, reaction of

Table 3: Steady-State Kinetic Parameters for Thioanisole Sulfoxidation in the Presence of Mixtures of Various Hemo-proteins and H_2O_2 [a]

protein	K_m (M)	V_{max} (s^{-1})	turnover no. (s^{-1})	% ee $R(+)$	source
wild-type human Mb	3.4×10^{-4}	9.2×10^{-4}	18	33 (4)[b]	this study
Y103F Mb	5.8×10^{-4}	4.1×10^{-4}	8.2	6 (3)[b]	this study
HRP	0.56×10^{-3}	23×10^{-3}	940	70	(*36, 51*)

[a] Reaction conditions were as described under Experimental Procedures. The absolute stereochemistry of the predominant sulfoxide was determined to be *R*(+) by polarimetery. [b] Percent enantiomeric excess (% ee) is presented as the mean ± SD, $n = 5$, and determined by assessing the *R*(+)- and *S*(−)-thioanisole sulfoxide distribution under all conditions examined.

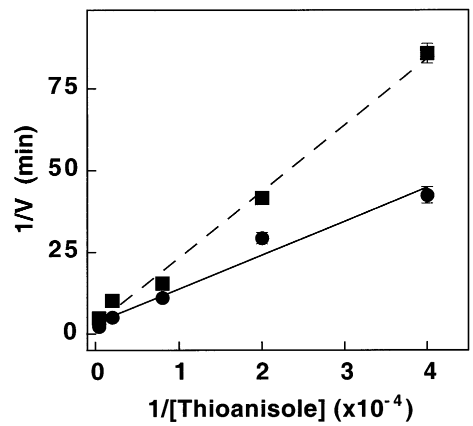

FIGURE 7: Double-reciprocal plots of the steady-state yield of thioanisole sulfoxide. Thioanisole (at the concentrations indicated) was treated with either 50 μM wild-type Mb (circles) or Y103F variant Mb (squares) and H_2O_2 (H_2O_2:Mb ∼10 mol/mol) in phosphate buffer (50 mM, pH 6, at 37 °C). After incubation for 1 h, the yield of thioanisole sulfoxide in the reaction mixture was determined by HPLC as described under Experimental Procedures.

the Y103F variant/H_2O_2 and thioanisole gave thioanisole sulfoxide as a racemic mixture (Figure 6 and Table 3). Double-reciprocal plots of reaction rate against thioanisole concentration (Figure 7) afforded linear relationships for the wild-type Mb and Y103F variant Mb, yielding the corresponding K_m and V_{max} values (Table 3). Values of V_{max} and K_m were decreased and increased, respectively, upon mutation of Y103, reflecting the lower k_1 value for the reaction of this variant Mb with H_2O_2. These values were also significantly lower than the steady-state parameters reported for HRP-mediated thioanisole sulfoxidation (*36, 51*). Similarly, and consistent with the limited ability of Mb for peroxidase activity, turnover numbers for the Mb proteins investigated were significantly lower than the corresponding value for HRP (Table 3).

DISCUSSION

It is commonly assumed that eliminating pathways of intramolecular electron transfer within the Mb active site will enhance peroxidase activity. In direct contrast to the expectation that inhibition of globin$^\bullet$ radical formation on Mb results in an enhanced peroxidase activity for this protein, the data presented herein indicate that mutation of Y103 effectively decreases the activity of this protein toward H_2O_2. This conclusion is supported by a marginal decrease in the absolute rate constant for reaction of the Y103F variant Mb with H_2O_2 and a corresponding decrease in the V_{max} value for thioansole sulfoxidation. In addition, the increased K_m value obtained for the reaction of Y103F Mb and thioansiole sulfoxide indicates a weaker substrate binding. The latter is completely consistent with the significant decrease in stereospecificity for thioanisole sulfoxidation compared to the corresponding wild-type control. Also, C110 in human Mb can act as a radical sink, yielding C110-thiyl radicals in the presence of peroxide (*28*). While the C110A mutation prevents thiyl radical formation on human Mb (*28*), the rate constant for the reaction of protein and peroxide was not different from that of the wild-type control. Thus, amino acid modification within the active site can have a bearing on the reaction of peroxide with Mb, while point mutations at the periphery of the protein are inconsequential to this activity. Overall, the new data indicate that the elimination of pathways leading to electron translocation (through mutation of oxidizable amino acids within the heme pocket) is not the sole determinant for enhancing Mb peroxidase activity.

Molecular engineered Mb proteins have, in general, produced disappointing results in terms of enhancing catalytic activity. Unlike authentic peroxidase enzymes, the heme-iron center of ferric Mb is generally hexa-coordinated except for the reduced deoxygenated state. H64 is a conserved residue located in the distal ligand-binding site of all mammalian Mb proteins (Figure 1). H64 plays a major role in stabilizing coordinated oxygen, water (as the sixth ligand), or other ligands through hydrogen bonding, as well as actively participating in acid−base catalysis. Studies with a series of H64 Mb variants unambiguously showed that H64 plays a key role in the catalytic activity of the protein (*23*). Thus, a simplistic approach suggests that mutation of H64 may engineer Mb to exhibit comparable activity to authentic peroxidases. However, H64 variants of sperm whale Mb showed only modest (∼1.5−30-fold) increases in peroxidase activity (*23*, *52*). Furthermore, the absolute rate constants for these engineered proteins consistently remained 3−4 orders of magnitude lower than that for an authentic peroxidase (e.g., HRP, $k_1 \sim 10^7\ M^{-1}\ s^{-1}$) (*53*, *54*). The presence or absence of suitable reducing agents on the matrix adjacent to the heme prosthetic group is a key determinant of whether the second oxidation equivalent is presented as an unstable porphyrin π-radical cation or as a globin$^\bullet$ derived from the oxidation of the protein matrix (*11*, *54*).

Paradoxically, improved peroxidase activity is obtained with yet other Mb variants that introduce an electron-rich (oxidizable) amino acid at F43 [i.e., F43H (*42*), F43Y (*55*), and F43W (*25*)]. Similarly, random mutagenesis has successfully identified a T39I/K45D/F46L/I107F variant Mb with increased peroxidase activity (*6*). Despite the 25-fold greater activity of the quadruple variant than the wild-type protein, the enhanced catalytic activity remained significantly lower than the intrinsic activity of authentic peroxidases. The difficulty in interpreting the available data indicates that a clear strategy is yet to be established that will yield an engineered Mb with catalytic activity comparable to authentic peroxidases.

Previous EPR studies using spin-trapping agents have indicated that hydroxyl radicals are not produced from reactions of H_2O_2 with either human (*28*, *32*) or equine (*56*) Mb. These data effectively rule out the possibility that this reactive oxidant is responsible for the formation of globin$^\bullet$ on Mb through direct oxidation of the protein. Therefore, the evidence obtained in this study supports the conclusion that wild-type and Y103F variant human Mb proteins react with peroxide through a heterolytic mechanism generating ferryl Mb and water in the process. However, mammalian myoglobins (e.g., wild-type and variant sperm whale Mb) may react with other organic peroxides by both homolytic and heterolytic mechanisms (*11*). For the case of organic peroxides, the extent of heterolysis depends on the pK_a (*57*) of the alcohol produced from the degradation reaction while the extent of homolysis is apparently dependent on the stability of the radical produced from the β-scission reaction of the corresponding alkoxyl radical (*58*).

Definitive assignment of a tyrosyl phenoxyl radical to protein radicals is complicated by the fact that tyrosyl radicals exhibit variable EPR hyperfine signal structure. Hyperfine couplings vary, depending on the conformation of the side chain (in particular C−H_α) relative to the π-system of the phenol group. Thus, tyrosyl radicals reportedly exhibit two- (*59*) or multi-line EPR spectra (*60*), resulting from decreased and increased overlap of electronic orbitals, respectively. In general, the extent of orbital overlap is dictated by the degree of steric constraint applied to the phenyl ring of tyrosine by other nearby residues. Assignment of a tyrosyl phenoxyl radical to the multiplet EPR signal detected in reactions of Y103F Mb with H_2O_2 (Figure 3F) indicates that the plane of the phenyl ring is orientated to facilitate electron delocalization throughout the aromatic π-system and the σ-bonding orbitals of the benzylic (C−H_α) position.

Interestingly, the tyrosyl radical detected from samples of Y103F Mb/H_2O_2 is generated simultaneously with W14-OO$^\bullet$ in the presence of excess peroxide. In contrast, tyrosyl radicals are detected only after the decay of W14-OO$^\bullet$ in the corresponding reactions of sperm whale (*19*, *20*), horse (*43*), and human Mb (*28*). The sequential formation of W14- and then Y103/146-derived radicals has been interpreted as support for the idea that radical transfer can occur between these amino acids either by intra- or by intermolecular mechanisms. Furthermore, that long-range electron transfer between tryptophan and tyrosine has been reported (reviewed in *61*) and that W14-OO$^\bullet$ is capable of reacting with tyrosine residues on other proteins (*62*) are taken as further support for the idea that W14- and then Y103/146-derived radicals interact through either intra- or intermolecular mechanisms. Alternatively, the signal assigned to Y103/146-derived radicals may be obscured by the W14-OO$^\bullet$ radical and become increasingly resolved upon decay of the peroxyl radical to below detection limits. Yet another explanation is that an electron-transfer process between Y103/Y146 may result in line broadening on the EPR time-scale and account for the broad EPR signal detected after the decay of W14-OO$^\bullet$. Interestingly, the phenoxyl radical on Y103F Mb is well-resolved, exhibits fine structure, and represents ∼58% of the total tyrosyl radical concentration detected in the corresponding reactions of wild-type and C110A variant proteins. This can be interpreted as support for the idea that mixtures of Y103- and Y146-derived tyrosyl radicals coexist simultaneously on the wild-type protein and these radicals yield closely overlapping unresolved EPR signals.

Previously we determined that the pK_a value for the Y103F variant was significantly lower than that of the wild-type protein (*32*). The decrease in pK_a value for the acid−base transition of Y103F Mb indicates that the point mutation likely introduces a subtle change to the heme pocket that alters the binding of the water ligand to the ferric iron center. This minor change may involve a redistribution of the hydrogen-bonding network in the heme pocket as structural changes were not detected by either circular dichroism spectroscopy (*32*) or EPR analyses of the various resting-state proteins as determined in the present study. Importantly, the observed decrease in stereospecificity of thioanisole sulfoxidation catalyzed by the Y103F variant Mb is consistent with a putative alteration to the hydrogen-bonding network within the Mb active site that results in weaker binding and a greater degree of freedom to the substrate. Together, these data support the idea that the close proximity of Y103 to the heme-edge allows this residue to play an active role in binding and orientation of both exogenous substrates (e.g., thioanisole) and ligands (e.g., water) within the heme pocket of Mb. Future studies comparing structural elements of the heme pocket in both the wild-type and variant proteins by use of X-ray absorption fine structure spectroscopy may provide further evidence to substantiate this idea.

In summary, enhancement of Mb peroxidase activity based on site-directed molecular engineering leads to unpredictable results. Furthermore, the cumulative results to date indicate that molecular engineering of Mb has yielded a range of changes to Mb peroxidase activity (including both positive and negative enhancements). Despite these conflicting results, data obtained from engineered Mb have afforded a better understanding of the roles of specific amino acids in the catalytic activity of the protein. The Y103F mutation in human Mb successfully modulated globin$^{\bullet}$ radical formation on Mb, but it resulted in decreased (rather than increased) catalytic activity as assessed by both rapid kinetic and steady-state analyses. Overall, the results point to the importance in understanding not only the roles of protein radicals in the transfer of oxidizing equivalents but also the role of individual amino acid residues around the heme pocket in stabilizing the catalytic intermediates through steric and hydrogen-bonding effects. Clearly both are important contributing factors in understanding the properties of authentic peroxidases as well as the design of engineered protein catalysts.

ACKNOWLEDGMENT

We thank Prof. Roland Stocker and Dr. Aviva Levina for numerous helpful discussions and Prof. Steven G. Boxer and Dr. Eunice Park for providing the plasmids used to express wild-type human Hb and the C110A variant.

REFERENCES

1. Everse, J., Everse K. E., and Grisham, M. B. (1991) *Peroxidases in Chemistry and Biology*, Vol. I and II, CRC, Boca Raton, FL.
2. Welinder, K. G. (1992) *Curr. Opin. Struct. Biol. 2*, 388−393.
3. Dunford, H. B. (1999) in *Heme Peroxidases*, John Wiley and Sons, New York.
4. Widersten, M., and Mannervik, B. (1995) *J. Mol. Biol. 250*, 115−122.
5. Kwon, K. S., Kim, J., Shin, H. S., and Yu, M. H. (1994) *J. Biol. Chem. 269*, 9627−9631.
6. Wan, L., Twitchett, M. B., Eltis, L. D., Mauk, A. G., and Smith, M. (1998) *Proc. Natl. Acad. Sci. U.S.A. 95*, 12825−12831.
7. Wittenberg, B. A., and Wittenberg, J. B. (1989) *Annu. Rev. Physiol. 51*, 857−878.
8. Qiu, Y., Sutton, L., and Riggs, A. F. (1998) *J. Biol. Chem. 273*, 23426−23432.
9. Lloyd-Raven, E., and Mauk, A. G. (2000) *Adv. Inorg. Chem. 51*, 1−49.
10. George, P., and Irvine D. H. (1952) *Biochem. J. 52*, 511−517.
11. Allentoff, A. J., Bolton, J. L., Wilkis, A., Thompson, J. A., and Ortiz de Montellano, P. R. (1992) *J. Am. Chem. Soc. 114*, 9744−9749.
12. Rao, S. I., Wilks, A., and Ortiz de Montellano, P. R. (1993) *J. Biol. Chem. 268*, 803−809.
13. Tew, D., and Ortiz de Montellano, P. R. (1988) *J. Biol. Chem. 263*, 17880−17886.
14. Davies, M. J. (1991) *Biochim. Biophys. Acta 1077*, 86−90.
15. DeGray, J. A., Gunther, M. R., Tschirret-Guth, R., Ortiz de Montellano, P. R., and Mason, R. P. (1997) *J. Biol. Chem. 272*, 2359−2362.
16. Matsui, T., Ozaki, S., and Watanabe, Y. (1997) *J. Biol. Chem. 272*, 32735−32738.
17. Ozaki, S., Roach, M. P., Matsui, T., and Watanabe, Y. (2001) *Acc. Chem. Res. 34*, 818−825.
18. Ozaki, S., Hara, I., Matsui, T., and Watanabe, Y. (2001) *Biochemistry 40*, 1044−1052.
19. Villegas, J. A., Mauk, A. G., and Vazquez-Duhalt, R. (2000) *Chem. Biol. 7*, 237−244.
20. Wittenberg, J. B. (1970) *Physiol. Rev. 50*, 559−636.
21. Merx, M. W., Flögel, U., Stumpe, T., Gödecke, A., Decking, U. K. M., and Schrader, J. (2001) *FASEB J. 15*, 1077−1079.
22. Garry, D. J., Ordway, G. A., Lorenz, J. N., Radford, N. B., Chin, E. R., Grange, R. W., Bassel-Duby, R., and Williams, R. S. (1998) *Nature 395*, 905−908.
23. Gödecke, A., Flögel, U., Zanger, K., Ding, Z., Hirchenhain, J., Decking, U. K., and Schrader, J. (1999) *Proc. Natl. Acad. Sci. U.S.A. 96*, 10495−10500.
24. Garry, D. J., Meeson, A., Yan, Z., and Williams, R. S. (2000) *Cell. Mol. Life Sci. 57*, 896−898.
25. Brunori, M. (2001) *Trends Biochem. Sci. 26*, 290−292.
26. Flögel, U., Merx, M. W., Gödecke, A., Decking, U. K. M., and Schrader, J. (2001) *Proc. Natl. Acad. Sci. U.S.A. 98*, 735−739.
27. Hubbard, S. R., Hendrickson, W. A., Lambright, D. G., and Boxer, S. G. (1990) *J. Mol. Biol. 213*, 215−218.
28. Witting, P. K., Douglas, D. J., and Mauk, A. G. (2000) *J. Biol. Chem. 275*, 20391−20398.
29. Witting P. K., Douglas D. J., and Mauk A. G. (2001) *J. Biol. Chem. 276*, 3991−3998.
30. Takano, T. (1977) *J. Mol. Biol. 110*, 537−568.
31. Evans, S. V., and Brayer, G. D. (1988) *J. Biol. Chem. 263*, 4263−4268.
32. Witting, P. K., and Mauk, A. G. (2001) *J. Biol. Chem. 276*, 16540−16547.
33. Buettner, G. R. (1990) *Methods Enzymol. 186*, 125−127.
34. Zoller, M. J., and Smith, M. (1987) *Methods Enzymol. 154*, 329−350.
35. Varadarajan, R., Szabo, A., and Boxer, S. G. (1985) *Proc. Natl. Acad. Sci. U.S.A. 82*, 5681−5684.
36. Harris, R. Z., Newmyer, S. L., and Ortiz de Montellano, P. R. (1993) *J. Biol. Chem. 268*, 1637−1645.
37. Lay, P. A., and Levina, A. (1996) *Inorg. Chem. 35*, 7709−7717.
38. Antonini, E., and Brunori, M. (1971) in *Hemoglobin and Myoglobin in Their Reactions with Ligands*, North-Holland Publishing Co., Amsterdam, Holland.
39. Ikeda-Saito, M., Hori, H., Andersson, L. A., Prince, R. C., Pickering, I. J., George, G. N., Sanders, C. R., Jr., Lutz, R. S., McKelvey, E. J., and Mattera, R. (1992) *J. Biol. Chem. 267*, 22843−22852.
40. Teale, F. W. J. (1959) *Biochim. Biophys. Acta 35*, 543−548.
41. Wilks, A., and Ortiz de Montellano, P. R. (1992) *J. Biol. Chem. 267*, 8827−8833.
42. Ozaki, S., Matsui T., and Watanabe, Y. (1997) *J. Am. Chem. Soc. 119*, 6666−6667.
43. Gunther, M. R., Tschirret-Guth, R. A., Witkowska, H. E., Fann, Y. C., Barr, D. P., Ortiz De Montellano, P. R., and Mason R. P. (1998) *Biochem. J. 330*, 1293−1299.
44. Catalano, C. E., Choe, Y. S., and Ortiz de Montellano, P. R. (1989) *J. Biol. Chem. 264*, 10534−41051.

45. Holt, S., Reeder, B. J., Wilson, M., Harvey, S., Morrow, J. D., Roberts, L. J., Jr., and Moore, K. (1999) *Lancet 353*, 1241.
46. Osawa, Y., and Williams, M. S. (1996) *Free Radical Biol. Med. 21*, 35−41.
47. Reeder, B. J., and Wilson, M. T. (2001) *Free Radical Biol. Med. 30*, 1311−1318.
48. Khan, K. K., Mondal, M. S., Padhy, L., and Mitra, S. (1998) *Eur. J. Biochem. 257*, 547−555.
49. Matsui, T., Ozaki, S., Liong, E., Phillips, G. N., Jr., and Watanabe, Y. (1999) *J. Biol. Chem. 274*, 2838−2844.
50. Egawa, T., Shimada, H., and Ishimura, Y. (2000) *J. Biol. Chem. 275*, 34858−34866.
51. Ozaki, S., and Ortiz de Montellano, P. R. (1995) *J. Am. Chem. Soc. 117*, 7056−7061.
52. Brittain, T., Baker, A. R., Butler, C. S., Little, R. H., Lowe, D. J., Greenwood, C., and Watmough, N. J. (1997) *Biochem. J. 326*, 109−115.
53. Dolman, D., Newell, G. A., Thurlow, M. D., and Dunford, H. B. (1975) *Can. J. Biochem. 53*, 495−501.
54. Miller, V. P., Goodin, D. B., Friedman, A. E., Hartmann, C., and Ortiz de Montellano, P. R. (1995) *J. Biol. Chem. 270*, 18413−18419.
55. Levenger, D. C., Steveson, J.-A., and Wong, L.-L. (1995) *J. Chem. Soc., Chem. Commun.*, 2305−2306.
56. Turner, J. J., Rice-Evans, C. A., Davies, M. J., and Newman, E. S. (1991) *Biochem. J. 277*, 833−837.
57. Lee, W. A., and Bruice, T. C. (1985) *J. Am. Chem. Soc. 107*, 513−514.
58. Barr, D. P., Martin, M. V., Guengerich, F. P., and Mason, R. P. (1996) *Chem. Res. Toxicol. 9*, 318−325.
59. Borg, D. G. (1967) in *Biological Applications of Electron Spin Resonance* (Swartz, H. M., Bolton, J. R., and Borg, D. G., Eds.) pp 265−350, Wiley-Interscience, New York.
60. DeGray, J. A., Lassmann, G., Curtis, J. F., Kennedy, T. A., Marnett, L. J., Eling, T. E., and Mason, R. P. (1992) *J. Biol. Chem. 267*, 23583−23588.
61. Davies, M. J., and Dean, R. T. (1997) *Radical Mediated Protein Oxidation: From chemistry to medicine*, Oxford University Press, Oxford U.K.
62. Irwin, J. A., Ostda, H., and Davies, M. J. (1999) *Arch. Biochem. Biophys. 362*, 94−104.
63. Loo, S., and Erman, J. E. (1975) *Biochemistry 14*, 3467−3470.

BI025835W